DESIGN AND SIMULATION OF QUADRILATERAL RELAYS IN AC TRANSMISSION LINES WITH VSC-BASED HVDC SYSTEMS UNDER PHASE-TO-GROUND FAULT CONDITION

M. MOHAN[1], K. PANDURANGA VITTAL[2]

Voltage source converters (VSC)-based high voltage direct current (HVDC) transmission system can be used to integrate the offshore wind power generation with an AC grid. Due to the interconnection of VSC-HVDC system with the AC grid, an operation of distance relays might get affected. Also, fault resistance plays a significant role in the performance of ground relays. The ground faults have higher fault resistance causes the accuracy of the ground relay gets affected significantly. In this paper, the three-zone quadrilateral characteristic-based distance relay is designed to protect the AC transmission lines under phase-to-ground fault with fault resistance. Simulation studies are carried out to test the performance of the quadrilateral relay under phase-to-ground fault including various fault resistance cases in an AC transmission line with the effect of VSC-HVDC system. The impact of the dynamic conditions of the VSC-HVDC system on the performance of the quadrilateral relays under phase-to-ground fault with fault resistance cases is presented. Also, the performance comparison of the quadrilateral relay with the mho relay under such conditions is presented.

Keywords: Ground Faults, Distance Relays, High Voltage Direct Current (HVDC), Voltage Source Converters (VSC).

1. Introduction

Under the present scenario in power system, developing a protection scheme for AC transmission line is very challenging since the power electronics devices such as flexible AC transmission systems (FACTS) and voltage source converters (VSC)-based high voltage direct current (HVDC) systems are penetrated to the AC system due to the requirement of high-power renewables integration with the existing AC grid.

The fault resistance affects the performance of the distance relay since the distance between the relay location and fault point is not necessarily proportional

[1] Research Scholar, Department of Electrical and Electronics Engineering, National Institute of Technology Karnataka (NITK), Surathkal, Mangalore, Karnataka, India – 575025. e-mail: mohanbe.m@gmail.com

[2] Professor, Department of Electrical and Electronics Engineering, National Institute of Technology Karnataka (NITK), Surathkal, Mangalore, Karnataka, India – 575025.

to the impedance seen by the relay. In such condition, the conventional distance relay cannot give the accurate fault detection in an AC transmission line.

The numerical relay can be applied for the protection of high voltage (HV) transmission line since the conventional distance relay takes the decision based on the local measurements only such as AC voltage and current measured at the relay location. Therefore, the numerical relay with quadrilateral characteristics might be an excellent option to protect the AC transmission line where the resistance and reactance can be altered according to the system.

The authors of [1] have proposed a new compensation method to avoid the underreach problem for ground relays based on the calculation of fault resistance. Also, the performance of the quadrilateral characteristic-based relay is analysed in a 500-kV power system under symmetrical and unsymmetrical fault cases with the effect of fault resistance up to 300 Ω using electromagnetic transients' program (EMTP). In [2], a new Bergeron distance relay scheme is presented for the 1000-kV ultra-high voltage (UHV) line using the distributed parameter line model.

In [3], the performance of the mho and quadrilateral characteristic-based relays are analysed under faults with different fault resistance in an IEEE 39 bus 10 generator test system using PSCAD/EMTDC simulation. The new method for resistive reach setting of quadrilateral characteristics is presented in [4]. The authors of [5] have proposed a new adaptive distance protection scheme based on the complex impedance plane, which is immune to the fault resistance, applicable to the various type of faults and adaptable to different operating conditions in a 500-kV transmission system.

In [6], the performance of the mho characteristic-based distance relay has analysed in a 400-kV transmission line with static var compensators (SVC) such as thyristor-controlled reactor (TCR) and thyristor switched capacitor (TSC). The authors of [7] have presented the effect of unified power flow controller (UPFC) on the performance of the mho and quadrilateral characteristic relays in a 230-kV transmission line. It was showed that the mho relay gives the underreaching and overreaching problems under high resistance fault on a UPFC compensated lines where the quadrilateral relay provides better performance. However, the quadrilateral relay also mal-operates under the case of very high fault resistance and capacitive reactive power exchange via UPFC. In such cases, it was suggested that the adaptive methods might provide a better solution to the compensated transmission line.

Researchers [8]–[10] have presented the impact of HVDC system on distance protection of transmission line. However, the dynamic operating conditions of the VSC-HVDC system and its influence on the performance of the distance relay is not reported. The authors of [11] have evaluated the performance of the distance relay with the effect of VSC-based HVDC system including the

dynamic operating conditions of the VSC. But it was used the mho characteristic-based distance relay which is not suitable for the phase-to-ground fault with high resistance cases. References [12]–[14] have analysed the dynamic impact of the VSC-HVDC system on the quadrilateral characteristic-based distance relay in an AC transmission line. However, the reach setting of the quadrilateral characteristics might be different for the phase and ground fault relays since the variation of the fault resistance is more significant for the phase-to-ground fault cases when compared to the phase-to-phase fault cases.

In this paper, the quadrilateral characteristic-based distance relay is designed, and its simulation studies are carried out to test the performance under phase-to-ground fault with the consideration of fault resistance up to 100 Ω in an AC transmission line with the effect of VSC-based HVDC transmission system. In addition, the impact of the dynamic conditions of the VSC-HVDC system on the performance of the quadrilateral relays under phase-to-ground fault with fault resistance cases is presented. Also, the comparison of the quadrilateral relays with the mho relays under such conditions are presented.

2. Study System

The 3-bus system with VSC-based HVDC transmission system linked offshore wind farm is shown in Fig. 1.

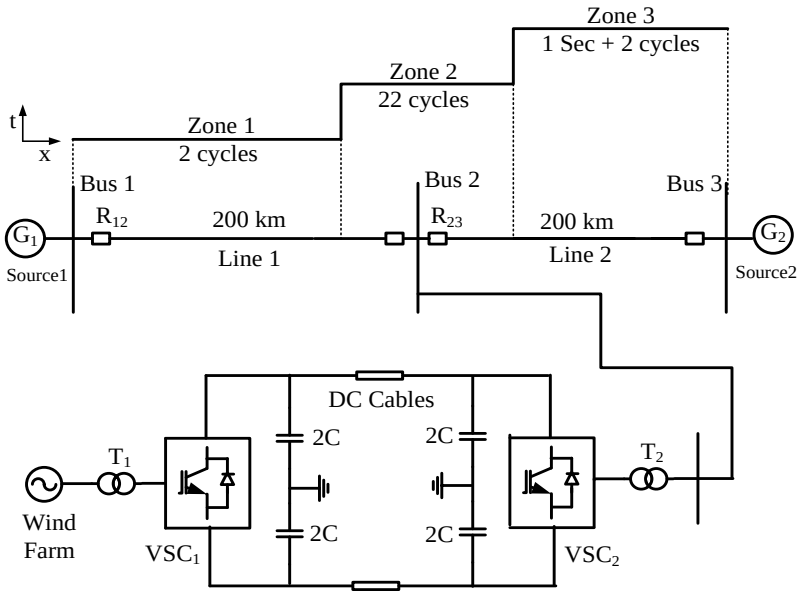

Fig. 1. 3-bus system with VSC-HVDC linked offshore wind farms.

In this test system, the 420 kV, 50 Hz source connected each other via the 3-bus system. The load angle between the two sources is 20˚. The length of each

transmission line (i.e., Line 1 and 2) is 200 km. The distance relay R_{12} is located in-between bus-1 and bus-2. The offshore wind farms are connected to the bus-2 terminal of the 3-bus system through VSC-based HVDC system.

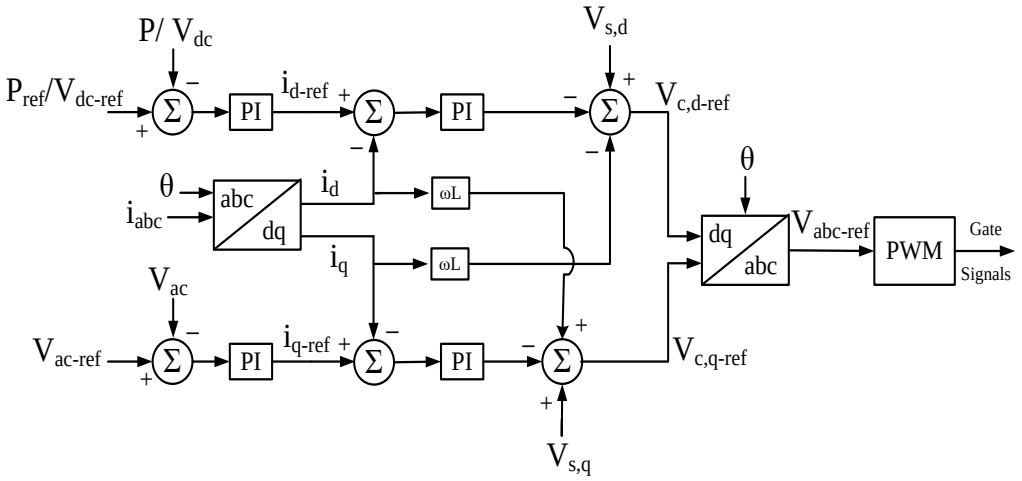

Fig. 2. Decoupled d-q control strategy for VSC-HVDC.

Fig. 2 shows the decoupled d-q control model for the two-level VSC which is used at both sides of the HVDC station (i.e., VSC_1 and VSC_2). The decoupled d-q control contains inner loop control which is independently controlling the active and reactive power, and outer loop control such as AC voltage (V_{ac}), active power (P) and DC voltage (V_{dc}) controller. In this control scheme, the d-axis of the rotor reference frame is aligned with the AC voltage vector, and q-axis is lagging d-axis by 90˚. The decoupled d-q control strategy is developed based on the following relations. The AC voltage (V_{ac}) in the d-q frame is given by,

$$V_{s,d} = Ri_d + L\frac{di_d}{dt} + \omega Li_q + V_{c,d} \tag{1}$$

$$V_{s,q} = Ri_q + L\frac{di_q}{dt} - \omega Li_d + V_{c,q} \tag{2}$$

where, $V_{c,d}$ and $V_{c,q}$ are the converter voltage in the d-q frame, i_d and i_q are the AC current in the d-q frame, and ω is the supply frequency. The active power (P) and DC voltage (V_{dc}) can be expressed by,

$$P = \frac{3}{2}\left(V_{s,d}i_d + V_{s,q}i_q\right) \tag{3}$$

$$P_{dc} = V_{dc}i_{dc} \tag{4}$$

where, i_{dc} is the DC current [15]–[18].

3. Design of Quadrilateral Relays

When the phase-to-ground fault occurs in a system, the fault resistance will be the considerable factors since it introduces an underreach problem in the distance relay. Numerical distance relay with the quadrilateral characteristics can be applied to protect the high voltage AC transmission line under such condition since the setting of the resistance and reactance of the characteristics can be altered accordingly. The three-zone quadrilateral characteristic-based distance relay is shown in Fig. 3. The design of the quadrilateral characteristics for Zone-1, Zone-2 and Zone-3 relay has been implemented with the help of references [2], [14], [19] and details of design procedure followed in presently is briefed following subsections.

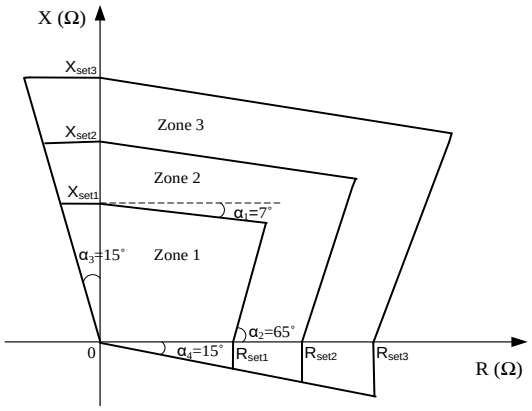

Fig. 3. Three-zone quadrilateral characteristic-based relay.

3.1 Zone-1 Setting

Consider the protection zones are designed for relay R_{12} which is indicated in Fig. 1. Zone-1 relay is designed to protect the 80% of the primary line (i.e., Line 1 as indicated in Fig. 1) without intentional time delay. The reactive reach of Zone-1 relay is considered as 80% reactance (0.8×X) of the primary line impedance (Z_{Line1}=R+jX). The resistive reach of Zone-1 relay consists of the 80 % resistance (0.8×R) of the primary line impedance and the additional resistive coverage of 70 Ω to overcome the problem of Zone-1 high resistance faults.

The reactance line in the first quadrant of the R-X plane is set to decline 7˚ (i.e., α_1=7˚) with respect to the resistance line in order to overcome the steady state overreach problem due to resistive faults. The relay characteristic is extended in the second and fourth quadrant of the R-X plane with the slope of 15˚ (i.e., α_3 and α_4 is 15˚) to perform the correct operation during close-in high resistance faults. The resistance line in the first quadrant of the R-X plane is designed with

the slope of 65˚ (i.e., α_2=65˚) to avoid incorrect tripping during high load conditions. The calculation used for zone-1 setting has given below:
The positive sequence impedance is given by,

$$z_1 = 0.423966868\angle 85.32710681^{\circ} \quad (5)$$

$$= (0.034539303 + j0.422557619)\ \Omega/\text{km} \quad (6)$$

The zero-sequence impedance is given by,

$$z_0 = 1.177029529\angle 75.34458819^{\circ} \quad (7)$$

$$= (0.297794508 + j1.138734799)\ \Omega/\text{km} \quad (8)$$

The positive sequence impedance for the Line 1 (i.e., 200 km) is given by,

$$= 200 \times (0.423966868\angle 85.32710681^{\circ})$$

$$= 84.7933736\angle 85.32710681^{\circ} \quad (9)$$

$$Z_{Line1} = R+jX = (6.907860686 + j84.51152387)\ \Omega \quad (10)$$

Using (9), Zone-1 reach setting is calculated by,

$$= 0.8 \times (84.7933736\angle 85.32710681^{\circ})$$

$$= 67.83469888\angle 85.32710681^{\circ}$$

$$= (5.526288549 + j67.6092191)\ \Omega \quad (11)$$

Reactive reach of Zone-1 relay (X_{set1}) is calculated by,

$$= (0.8 \times X) = 67.6092191\ \Omega \quad (12)$$

Resistive reach of Zone-1 relay (R_{set1}) is calculated by,

$$= (0.8 \times R) + 70\ \Omega = 75.526288549\ \Omega \quad (13)$$

3.2 Zone-2 Setting

Zone-2 relay is designed to protect the 120% of the primary line (i.e., Line 1 which is indicated in Fig. 1) with the time delay of 20 cycles (i.e., 0.4 seconds). The reactive reach of Zone-2 relay is considered as 120% reactance (1.2×X) of the primary line impedance (Z_{Line1}=R+jX). The resistive reach of Zone-2 relay consists of the 120 % resistance (1.2×R) of the primary line impedance and the additional resistive coverage of 100 Ω to cover the Zone-2 high resistance faults. The calculation used for the zone-2 setting has given below:
Using (9), Zone-2 reach setting is calculated by,

$$= 1.2 \times (84.7933736\angle 85.32710681^{\circ})$$

$$= 101.7520483\angle 85.32710681^{\circ}$$

$$= (8.289432822 + j101.4138286)\ \Omega \quad (14)$$

Reactive reach of Zone-2 relay (X_{set2}) is calculated by,

$$= (1.2 \times X) = 101.4138286\ \Omega \quad (15)$$

Resistive reach of Zone-2 relay (R_{set2}) is calculated by,

$$= (1.2 \times R) + 100\ \Omega = 108.289432822\ \Omega \quad (16)$$

3.3 Zone-3 Setting

Zone-3 relay is designed to protect the 220% of the primary line (i.e., Line 1 as indicated in Fig. 1) with the time delay of 1 second. The reactive reach of Zone-3 relay is considered as 220% reactance (2.2×X) of the primary line impedance (Z_{Line1}=R+jX). The resistive reach of Zone-3 relay consists of the 220 % resistance (2.2×R) of the primary line impedance and the additional resistive coverage of 200 Ω to cover the Zone-3 high resistance faults. The calculation used for the zone-3 setting has given below:

Using (9), Zone-3 reach setting is calculated by,

$$\begin{aligned} &= 2.2 \times (84.7933736\angle 85.32710681°) \\ &= 186.5454219\angle 85.32710681° \\ &= (15.19729351 + j185.9253525)\ \Omega \end{aligned} \quad (17)$$

Reactive reach of Zone-3 relay (X_{set3}) is calculated by,

$$= (2.2 \times X) = 185.9253525\ \Omega \quad (18)$$

Resistive reach of Zone-3 relay (R_{set3}) is calculated by,

$$= (2.2 \times R) + 200\ \Omega = 215.19729351\ \Omega \quad (19)$$

4. Simulation Studies

In this section, simulation studies are carried out to analyse the performance of the quadrilateral relays under the phase-to-ground fault in the 3-bus system with the effect of VSC-based HVDC transmission systems. The ground faults in all three zones are considered for the simulation study. Also, the effect of fault resistance on the quadrilateral relays and its comparison with the mho relay is presented. The simulation studies are carried out using PSCAD/EMTDC software.

4.1 Phase-to-Ground Fault condition

In this case, the performance of the Zone-1, Zone-2 and Zone-3 operation of the quadrilateral relay is analysed under phase A to ground (A-G) fault which occurs at 150 km, 230 km and 380 km distance from the relay R_{12} location (i.e., Bus-1 terminal) in the 3-bus system for both without and with VSC-HVDC cases. The performance of the quadrilateral relay R_{12} under A-G fault condition has shown in Fig. 4. Table 1 shows the apparent impedance measured by the relay R_{12} under A-G fault condition.

In case of fault on Zone-1 area of the relay R_{12}, the apparent impedance seen by the relay has not changed for both without and with VSC-HVDC cases. But in the case of fault on Zone-2 and Zone-3 area of the relay R_{12}, the apparent impedance seen by the relay has increased significantly when the VSC-HVDC is connected at the bus-2 terminal of the 3-bus system which can be seen from Fig. 4 and Table 1.

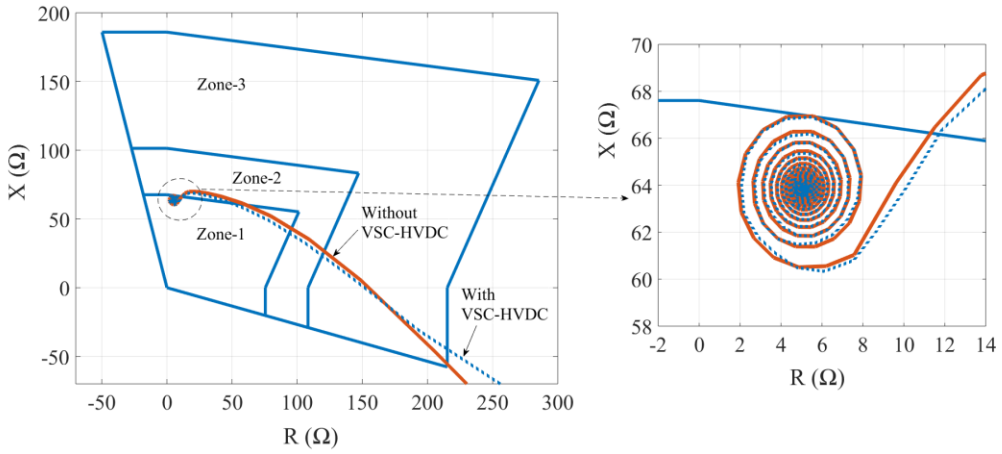

(a) Zone-1 fault (fault at 150 km distance from the relay location).

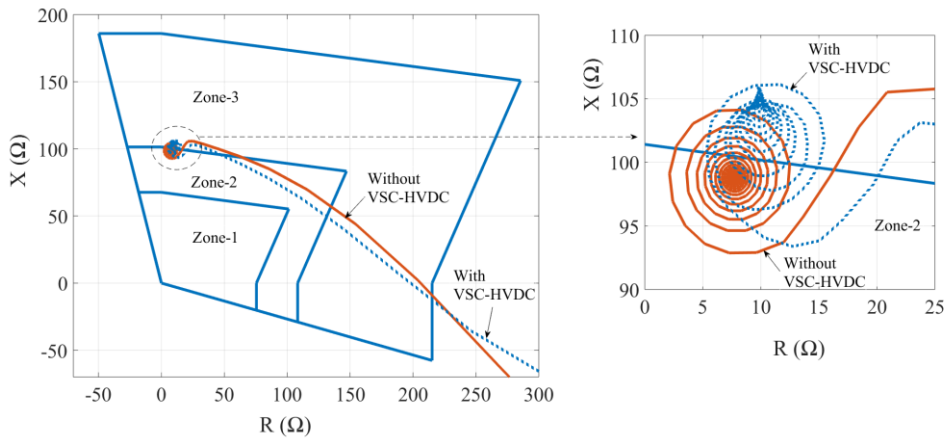

(b) Zone-2 fault (fault at 230 km distance from the relay location).

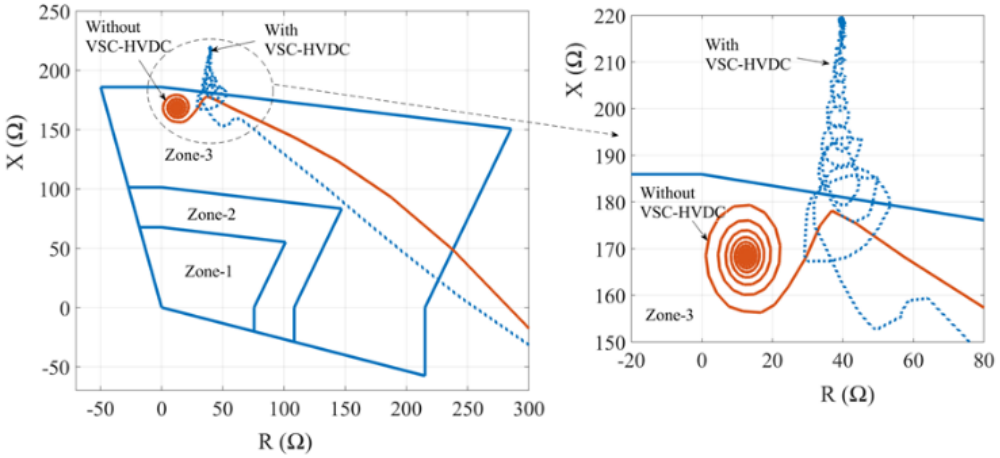

(c) Zone-3 fault (fault at 380 km distance from the relay location).

Fig. 4. The performance of the quadrilateral relay R_{12} under A-G fault in the 3-bus system for both without and with VSC-HVDC cases.

Table 1.

The apparent impedance (Z_a) seen by the relay R_{12} under A-G fault condition

Fault Location	Z_a (Ω) (without VSC-HVDC)	Z_a (Ω) (with VSC-HVDC)
Zone-1	64.08∠85.42˚	64.05∠85.44˚
Zone-2	99.10∠85.53˚	106.32∠84.72˚
Zone-3	168.82∠85.42˚	223∠79.68˚

Due to the interconnection of VSC-HVDC into the AC system, the impedance viewed by the relay for Zone-2 and Zone-3 fault has gone outside the Zone-2 and Zone-3 area of the relay which can lead to the maloperation of the relay. In such cases, adaptive reactive reach setting of the quadrilateral relay or adjusting the reactive power of VSC during fault period might work well since the reactive power of the AC network is varied due to the interconnection of VSC-HVDC system.

4.2 Step Change in VSC_2 AC voltage Reference Input during Phase-to-Ground Fault Condition

In this case, the performance of the Zone-2 and Zone-3 quadrilateral relay is analyzed under A-G fault at 230 km and 380 km distance from the relay location in the 3-bus system with VSC-HVDC and step variation of reference AC voltage (V_{acref}) of decoupled d-q control of grid side VSC (i.e., VSC_2) during fault period. The performance of the Zone-2 and Zone-3 relay has shown in Fig. 5.

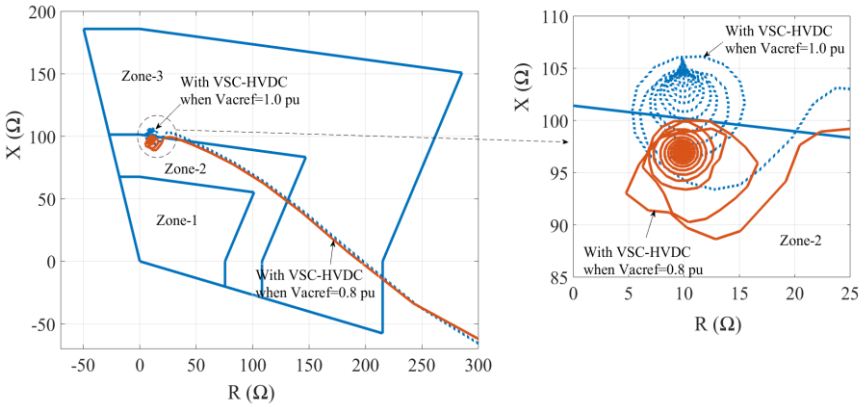

(a) Zone-2 fault (fault at 230 km distance from the relay location).

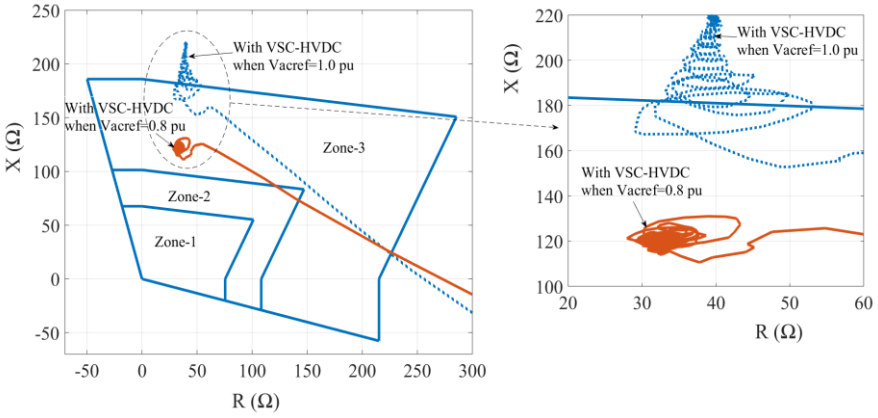

(b) Zone-3 fault (fault at 380 km distance from the relay location).

Fig. 5. The performance of quadrilateral relay R_{12} under A-G fault in the 3-bus system with VSC-HVDC and step variation of V_{acref} of VSC_2 from 1.0 to 0.8 per unit during fault period.

Table 2.

Apparent impedance (Z_a) seen by the relay R_{12} under A-G fault condition in the 3-bus system with VSC-HVDC.

Fault Location	Z_a (Ω) (V_{acref} = 1.0 per unit)	Z_a (Ω) (V_{acref} = 0.8 per unit)
Zone-2	106.32∠84.72˚	97.54∠84.19˚
Zone-3	223∠79.68˚	123∠74.81˚

When the V_{acref} is step changed from 1.0 to 0.8 per unit during fault period, the apparent impedance seen by the relay has reduced which can be seen from Fig. 5 and Table 2. Due to this reduction of apparent impedance measured by the relay, the impedance trajectory has located inside the protection zones. Therefore, Zone-2 and Zone-3 relay will issue the trip decision for the fault at 230

km and 380 km distance from the relay point. From the simulation results, it is observed that the maloperation of the backup relay can be resolved by altering the reactive power of the system using the variation of the reference AC voltage (V_{acref}) of decoupled d-q control of grid side VSC.

4.3 Phase-to-Ground Fault with Fault Resistance Effect on Mho and Quadrilateral Relay

4.3.1 Case 1: Zone-1 Fault

In this case, the performance of the Zone-1 mho and quadrilateral relay is analyzed under phase A to ground fault (A-G) with various fault resistance (R_f) which occurs at 150 km distance from the relay R_{12} location in the 3-bus system with VSC-HVDC. The fault resistance is considered as 0 to 100 Ω with 20 Ω increments for the simulation study. The comparison of Zone-1 mho and quadrilateral relay has shown in Fig. 6. For Zone-1 mho relay, 80 % of the primary line impedance has considered for the Zone-1 setting without intentional time delay.

The effect of fault resistance on the three-zone quadrilateral relay has shown in Fig. 6 (a). The impedance trajectory of all the fault cases (i.e., A-G fault with fault resistance varies from 0 to 100 Ω) falls within the relay characteristics. But, in the case of Zone-1 mho relay, the impedance trajectory of A-G fault with $R_f = 0$ Ω case only falls within the relay characteristics which is indicated in Fig. 6 (b). When fault resistance increases, the impedance trajectory has moved in the positive resistance axis which leads to the maloperation of the mho relay. In such cases, the Zone-1 quadrilateral relay has given better performance since the resistive reach of the characteristics has changed according to the system.

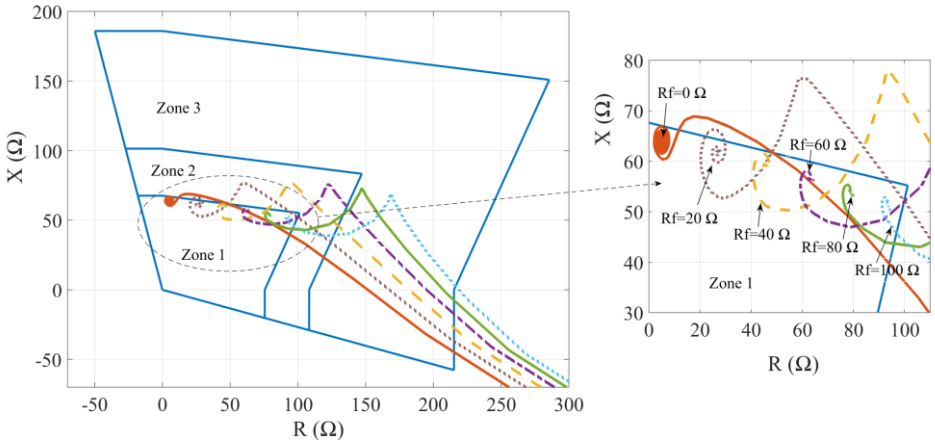

(a) Effect of fault resistance on three-zone quadrilateral relay.

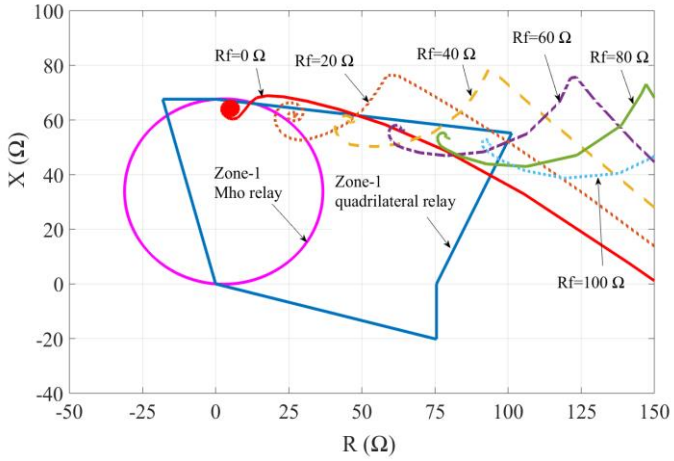

(b) Zone-1 mho and quadrilateral relay.

Fig. 6. Comparison of Zone-1 mho and quadrilateral relay R_{12} under A-G fault with various fault resistance (R_f) at 150 km distance from the relay location (Zone-1 area) in the 3-bus system with VSC-HVDC.

4.3.2 Case 2: Zone-2 Fault

In this case, the performance of the Zone-2 quadrilateral and mho relay is analyzed under the condition of A-G fault with various fault resistance which occurs at 230 km distance from the relay location in the 3-bus system with VSC-HVDC including the variation of V_{acref} of decoupled d-q control of VSC_2. Fig. 7 shows the performance of the Zone-2 relay under A-G fault with fault resistance varies from 0 to 100 Ω when the V_{acref} of VSC_2 is 1.0 per unit. For Zone-2 mho relay, 120 % of the primary line impedance is considered for the Zone-2 setting with 20 cycles delay.

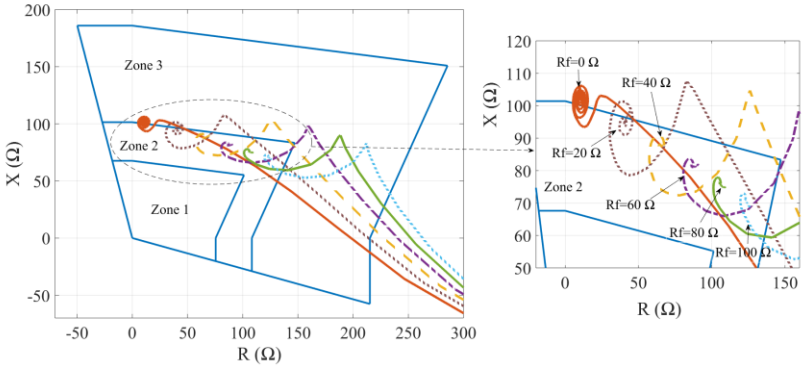

(a) Effect of fault resistance on three-zone quadrilateral relay.

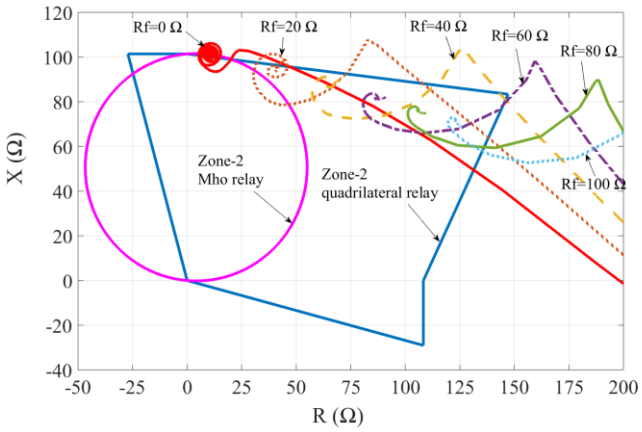

(b) Zone-2 mho and quadrilateral relay.

Fig. 7. Comparison of Zone-2 mho and quadrilateral relay R_{12} under A-G fault with various fault resistance (R_f) at 230 km distance from the relay location (Zone-2 area) in the 3-bus system with VSC-HVDC. (V_{acref}=1.0 per unit).

When the fault resistance increases, the impedance trajectory has falling inside the Zone-2 quadrilateral relay even the V_{acref} = 1.0 per unit which is indicated in Fig. 7 (a). The comparison of Zone-2 quadrilateral relay with the mho relay has presented in Fig. 7 (b). It demonstrates that the impedance trajectory has moved in the positive resistance axis of the R-X plane which is not locating inside the protection zone of the Zone-2 mho relay when the fault resistance increases. Also, the impedance trajectory for the fault with R_f = 0 **Ω** has not fallen inside the Zone-2 mho and quadrilateral relay.

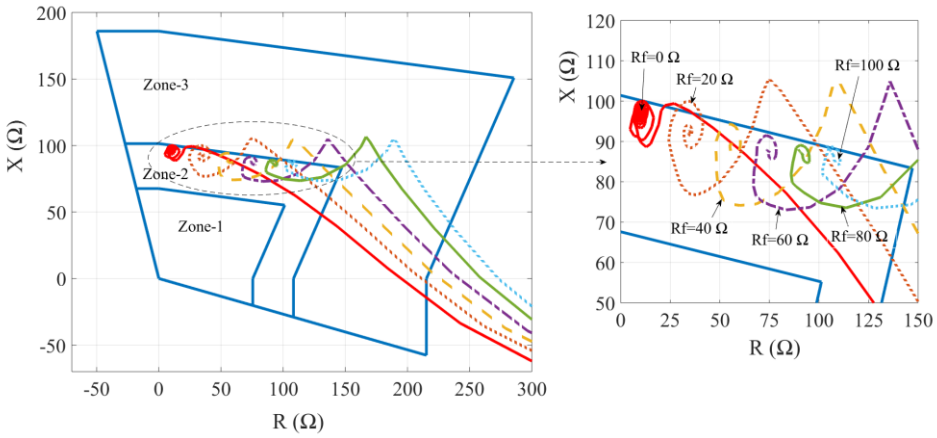

(a) Effect of fault resistance on three-zone quadrilateral relay.

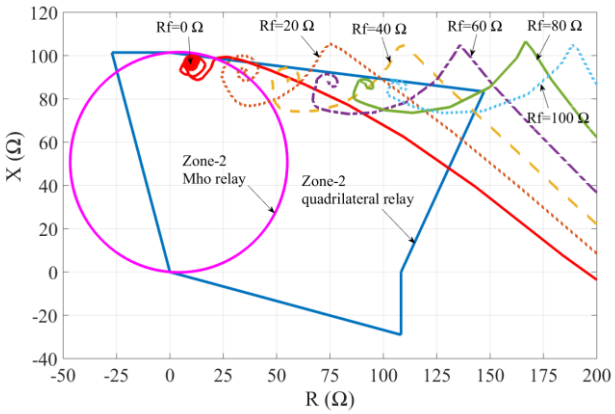

(b) Zone-2 mho and quadrilateral relay.

Fig. 8. Comparison of Zone-2 mho and quadrilateral relay R_{12} under A-G fault with various fault resistance (R_f) at 230 km distance from the relay location (Zone-2 area) in the 3-bus system with VSC-HVDC and step variation of V_{acref} of VSC_2 from 1.0 to 0.8 per unit during fault period.

The performance of the Zone-2 mho and quadrilateral relay has shown in Fig. 8 when the V_{acref} of VSC_2 is step varied from 1.0 to 0.8 per unit during fault period. The fault situation is similar to the previous case. In this case, the impedance trajectory for the fault with R_f = 0 **Ω** has fallen inside the protection zone which is indicated in Fig. 8 (a). Also, the decrement rate of the reactance value for different fault resistance case is very less when compared to the previous case due to the alteration of reactive power using the step variation of V_{acref} of grid side VSC (VSC_2) which can be observed from Fig. 7 (b) and 8 (b).

Table 3.

Comparison of apparent impedance (Z_a) seen by the Zone-2 relay R_{12} for different V_{acref} of VSC_2 under A-G fault with different fault resistance (R_f) at 230 km distance from the relay location.

R_f (Ω)	Z_a (Ω) with VSC-HVDC (V_{acref} = 1.0 per unit)	Z_a (Ω) with VSC-HVDC (V_{acref} = 0.8 per unit)
0	106.32∠84.72˚	97.54∠84.19˚
20	107.50∠65.89˚	98.63∠69.30˚
40	113.50∠52.19˚	105.20∠57.92˚
60	122.11∠42.10˚	114.75∠49.93˚
80	132.27∠34.46˚	125.59∠44.43˚
100	143.38∠28.69˚	136.75∠40.57˚

Table 3 shows the comparison of apparent impedance seen by the Zone-2 relay for different value of V_{acref} of VSC_2 under the condition of A-G fault with

various fault resistance which occurs at 230 km distance from the relay location in the 3-bus system with VSC-HVDC. When the V_{acref} is step changed from 1.0 to 0.8 per unit during fault period, the reactive power of the AC network has varied which can lead to the variation of apparent impedance seen by the relay. Hence, the Zone-2 relay R_{12} will trip the line for the fault which occurs on Zone-2 area even if the VSC-HVDC is connected in-between the relay location and fault point.

5. Conclusions

In this paper, the performance of the numerical distance relay is analysed in the 3-bus system with the effect of VSC-based HVDC transmission systems. The three-zone quadrilateral and mho relay are designed and modelled in PSCAD/EMTDC. Simulation studies are carried out to test the performance of the quadrilateral relay in the 3-bus system with the impact of VSC-HVDC system. From the simulation results, it is observed that the Zone-2 fault is moved to the Zone-3 area and Zone-3 fault has gone outside the boundary of the protection zones when the VSC-HVDC is connected at the bus-2 terminal of the 3-bus system. Therefore, the correct operation of the backup relay is performed by adjusting the reactive power of the system using the variation of the reference AC voltage (V_{acref}) of decoupled d-q control of VSC_2. In such cases, adaptive reactive reach setting of the quadrilateral relay also may give a better result. The performance of the quadrilateral relay is analysed and compared with the mho relay under the condition of ground fault with the effect of fault resistance which occurs on Zone-1, Zone-2 area of the relay in the 3-bus system with VSC-HVDC including the variation of V_{acref} of VSC_2. From the results, it is noticed that the impedance trajectory has located inside the protection zones of the quadrilateral relay even the fault resistance variation is a large value since the characteristics has altered accordingly. The obtained results indicate that the reactance value of the measured apparent impedance gets decreased when fault resistance increases due to the variation of reactive power which is caused by the interconnection of VSC-HVDC. The decrement rate of the reactance value of apparent impedance is reduced when the V_{acref} of VSC_2 is step changed from 1.0 to 0.8 per unit during the fault period. The studies can be extended to the larger network with the interconnection of the multi-terminal VSC-HVDC transmission system linked offshore wind farms. Also, the development of the adaptive distance relaying scheme for the AC grid with multi-terminal VSC-HVDC transmission system will be addressed in the future work since this paper has considered the manual control of the AC voltage reference input of decoupled d-q control of the VSC_2.

REFERENCES

[1] M. M. Eissa, “Ground distance relay compensation based on fault resistance calculation,” IEEE Trans. Power Del., vol. 21, no. 4, pp. 1830-1835, Oct. 2006.

[2] Z. Y. Xu, S. F. Huang, L. Ran, J. F. Liu, Q. X. Yang, and J. L. He, "A distance relay for a 1000-kV UHV transmission line," IEEE Trans. Power Del., vol. 23, no. 4, pp. 1795–1804, Oct. 2008.

[3] M. Harikrishna, "Development of quadrilateral relay for EHV/UHV lines," Master Thesis, Dept. Elect. Eng., Indian Institute of Technology, Roorkee, June 2010.

[4] E. Sorrentino, E. Rojas, and J. Hernández, "Method for setting the resistive reach of quadrilateral characteristics of distance relays," in Proc. 44th Int. Univ. Power Engineering Conf., Glasgow, U.K., 1-4 Sep. 2009, pp. 1–5.

[5] Ma, Jing, Xiaoqiang Xiang, Pei Li, Zhuojun Deng, and James S. Thorp, "Adaptive distance protection scheme with quadrilateral characteristic for extremely high-voltage/ultra-high-voltage transmission line," IET Generation, Transmission & Distribution, vol. 11, no. 7, pp. 1624-1633, June 2017.

[6] M. Zellagui, and A. Chaghi, "Impact of SVC devices on distance protection setting zones in 400 kV transmission line" UPB Scientific Bulletin, Series C: Electrical Engineering, vol. 75, no. 2, pp. 249-262, 2013.

[7] Chauhan, Nidhi, M. Tripathy, and R. P. Maheshwari, "Performance Evaluation of Mho and Quadrilateral Characteristic Relays on UPFC Incorporated Transmission Line," International Journal of Electronic and Electrical Engineering, vol. 7, no. 8, pp. 827-835, 2014.

[8] H. Wang, "The protection of transmission networks containing ac and dc circuits," Ph.D. Dissertation, University of Bath, 2014.

[9] L. He, and C. C. Liu, "Effects of HVDC connection for offshore wind turbines on AC grid protection," in Proc. 2013 IEEE Power and Energy Society General Meeting (PES), Vancouver, BC, Canada, 21-25 Jul. 2013, pp. 1-5.

[10] L. He, C. C. Liu, A. Pitto, and D. Cirio, "Distance Protection of AC Grid with HVDC-Connected Offshore Wind Generators," IEEE Trans. Power Del., vol. 29, no. 2, pp. 493-501, Apr. 2014.

[11] M. Mohan, and K. Panduranga Vittal, "Performance Evaluation of Distance Relay in the Presence of Voltage Source Converters-Based HVDC Systems," Journal of Electrical Engineering & Technology, vol. 14, no. 1, pp. 69-83, Jan. 2019.

[12] M. M. Alam, H. Leite, J. Liang, and A. da Silva Carvalho. "Effects of VSC based HVDC system on distance protection of transmission lines," International Journal of Electrical Power & Energy Systems, vol. 92, pp. 245-260, Nov. 2017.

[13] M. M. Alam, H. Leite, N. Silva, and A. da Silva Carvalho, "Performance evaluation of distance protection of transmission lines connected with VSC-HVDC system using closed-loop test in RTDS," Electric Power Systems Research, vol. 152, pp. 168-183, Nov. 2017.

[14] M. M. Alam, "Distance Protection of Networks Supplied from VSC-HVDC," Ph.D. Dissertation, University of Porto, Portugal, March 2018.

[15] M. Mohan, and K. Panduranga Vittal, "Modeling and simulation studies on performance evaluation of three-terminal VSC-HVDC link connected offshore wind farms," in Proc. IEEE International Conference on Energy, Communication, Data Analytics and Soft Computing (ICECDS), Chennai, India, 1-2 Aug. 2017, pp. 473-478.

[16] Snigdha Tale, M. Mohan, and K. P. Vittal, "Performance analysis of distance relay in an AC grid with VSC-HVDC connection," in Proc. IEEE International Conference on Intelligent Computing, Instrumentation and Control Technologies (ICICICT), Kannur, India, 6-7th July 2017, pp. 1363-1368.

[17] A. Manoloiu, and M. Eremia, "Aspects on control of a VSC-HVDC transmission link," UPB Scientific Bulletin, Series C: Electrical Engineering and Computer Science, vol. 78, no. 4, pp. 161-170, Jan. 2016.

[18] A. Ghalem, A. Tayeb, S. Attallah, and K. M. Abdeldjabbar, "Robust and modern control of VSC-HVDC," UPB Scientific Bulletin, Series C: Electrical Engineering and Computer Science, vol. 80, no. 2, pp. 167-180, Jan. 2018.

[19] Model setting calculations for typical IEDs line protection setting guidelines protection system audit checklist recommendation for protection management," India, 2014.